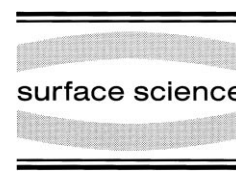




ELSEVIER

Surface Science 441 (1999) 140–148



www.elsevier.nl/locate/susc

# Metastable and excited states of the C defects of Si(001)

K. Hata, S. Ozawa, H. Shigekawa \*

*Institute of Applied Physics and CREST, Japan Science and Technology Corporation (JST), University of Tsukuba, Tennodai 1-1-1, Tsukuba 305-8573, Japan*

Received 8 January 1999; accepted for publication 30 July 1999

## Abstract

Dynamic characteristics of the C defect were studied by consecutive scanning tunneling microscopy observations. Not only the transformation of the C defect into a C2 defect but also the reverse transition, a C2 to C structural change, and a more complicated C to C2–C2 transformation were observed. All of the experimental results suggest that the C2 defect is a metastable and excited state of the C defect that has a similar electronic structure to the C defect. Extensive scanning tunneling spectroscopy measurements reveals that there exists several (at least two) types of C defect, which we believe to represent metastable states of the C defect. Our interpretation is that there are two atoms (probably silicon) in the top layer of the C defect which are weakly bound to the layer beneath, and possibly take several configurations. Each of the configurations is observed as a metastable state of the C defect. © 1999 Published by Elsevier Science B.V. All rights reserved.

*Keywords:* Scanning tunneling microscopy; Scanning tunneling spectroscopies; Silicon; Surface defects; Surface electronic phenomena

## 1. Introduction

The first scanning tunneling microscopy (STM) observation of a clean Si(001) surface, carried out by Tromp et al. [1] at room temperature, not only gave the first direct evidence of dimerization of the top-layer silicon atoms, but also showed that there exists a rather large number of atomic-scale defects on the surface. Subsequent STM observations of the clean Si(001) surface repeatedly showed certain amounts of defects. Hamers and Kohler classified these defects into three types, termed ‘A’, ‘B’ and ‘C’ defects [2].

Among these, the C defects are the most important. The C defects appear as two protrusions

along the dimer-row direction on one side of the dimer row and as a depression on the other side. The appearance of the protrusions is dependent on the surface voltage: they appear brighter than the surrounding dimers in empty-state STM images and darker in filled-state images taken at typical surface biases (ca.  $-2$  V) [2,3]. Other reported characteristics of the C defects are as follows. Tunneling current–voltage ( $I$ – $V$ ) measurements on the C defects show a metallic feature [2,4,5]. Regarding the rather high concentration of the C defects, they were supposed to be the prominent cause of Fermi-level pinning [2]. Frequently it is reported that the C defects influence the site of adsorption. For example, it is reported that the C defects are sensitive to oxidation [4,6,7]. These features make it clear that the C defects play a leading role in characterizing the surface [2], and therefore it is of critical importance to understand the characteristics of the C defect.

\* Corresponding author. Fax: +81-0298-55-7440;  
Internet: <http://dora.ims.tsukuba.ac.jp>.  
E-mail address: [hidemi@ims.tsukuba.ac.jp](mailto:hidemi@ims.tsukuba.ac.jp) (H. Shigekawa)

Some interesting features regarding the dynamic characteristics of the C defect have been reported by Zhang et al. [3]. They observed a frequent structure transformation of the C defect into another defect in two sequentially acquired STM images. The new defect was termed the C2 defect and was considered to be a variation of the C defect. The appearance of the C2 defect in the STM image is like one of the individual protrusions of the C defect being transferred to the opposite side of the dimer row.

In this paper we report our detailed study of the structural transformation of the C defects by STM and scanning tunneling spectroscopy (STS) measurements that yield new insights into our

understanding of the C defects. During the sequential STM observation of a single C defect, we observed not only the transformation of the C defect into a C2 defect but also the reverse transition, a C2 to C structural change, and a more complicated C to C2–C2 transition. Observations of both the C→C2 and the reverse C2→C transitions suggest that the C2 defect is a metastable and excited state of the C defect. At each stage, before and after the transition, we carried out STS measurements of the defects to resolve their electronic structures. We found that the C2 defect has a very similar electronic structure to the C defect even though their topographical appearance is quite different in the STM images, a result which

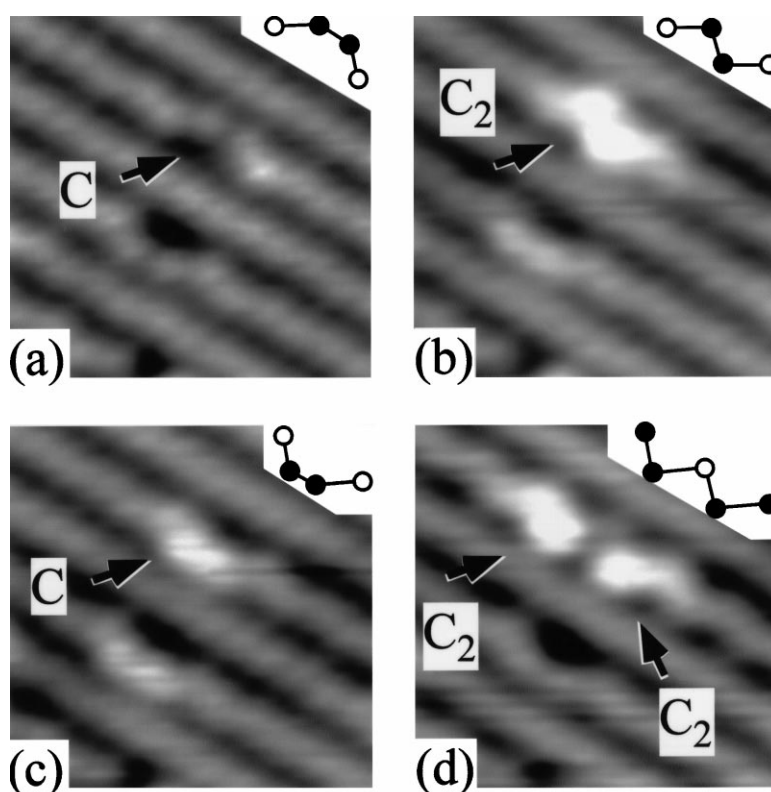


Fig. 1. A set of STM images showing the structural transformation of a C defect. Insets show stick and ball models of the structure of the C defect (black circles) and the surrounding dimers (white circles). (a) The initial surface. Two C defects are observed. The C defect indicated by the arrow showed the structural transformation. (b) An STM image taken 36 min later. The C defect has transformed into a C2 defect. (c) An STM image taken 57 min later. The C2 defect has recovered to a C defect. (d) An STM image taken 78 min later. A C to C2–C2 structural transformation was observed. Tunneling conditions were surface bias =  $-1.0$  V, current  $1$  nA. During the long intervals between the images shown, basically the same region was continuously scanned with a fresh rate of  $30$  s per image.

implies that the C2 defect is a close variation of the C defect. A simple structure model of the C defect is proposed based on the observed features of the C and C2 defects.

## 2. Experimental

Standard procedures were employed to fabricate the clean surface. Silicon samples were phosphorus-doped, with a conductivity of  $0.005 \Omega \text{ cm}$ . After the sample had been prebaked at  $\sim 700^\circ\text{C}$  overnight, it was flashed once to  $1250^\circ\text{C}$  for 30 s, followed by annealing at  $700^\circ\text{C}$  for another 30 s. The base pressure was kept below  $5 \times 10^{-8} \text{ Pa}$  during flashing. Electrochemically etched tungsten tips were used for the STM and STS measurements.

## 3. Results

### 3.1. Observation of the dynamic structural transition of the C defect

By continuous observations of identified C defects over a long time we studied the structural transformation of the C defect in detail. A set of subsequent STM images showing three consecutive structural transformations of a single C defect, which occurred in the course of a 1.5 h sequential observation, is displayed in Fig. 1 as an example. Fig. 1a shows the initial surface. Two identical C defects are observed, as indicated by the arrows. The first structural transformation occurred 36 min later, the C defect on the right transformed into a C2 defect as indicated by the arrow in Fig. 1b. This C to C2 structural transition was accomplished by transformation of the right protrusion of the right C defect to the opposite side of the dimer, in a fashion similar to that previously reported by Zhang et al. [3]. Note that the C2 defect appears brighter in the STM image at this surface bias than the C defect, which can be seen by comparing the C2 defect with the C defect on the left.

After 57 min, the second transition was observed as shown in Fig. 1c. A reverse procedure

of the first transition was observed and the C2 defect transformed into a C defect, a structural transition reported here for the first time. Careful analysis reveals that the recovered C defect is not exactly the same as the original C defect. This can be realized from two points: (1) the two protrusions of the original C defect were located on the right side of the dimer, while those of the recovered C defect are located on the left side; and (2) the intensity of the recovered C defect in the STM images is stronger than that of the original C defect. This can be understood by comparing the intensities of the recovered C defect and the original C defect. The recovered C defect appears brighter than the surrounding dimers, while the intensity of the original C defect is similar to that of the dimers. We frequently observed the C to C2 transition and the reverse C2 to C transition. As discussed later, observation of the C2 to C transition is very important to understand the characteristics of the C2 defect.

The final transition observed took place at 78 min, and the most complicated transformation was observed as shown in Fig. 1d. This transition occurred when we were carrying out an STS measurement on the recovered C defect; thus we believed that this transition was artificially induced. Indeed, this type of transition was not observed again. During the course of the transition, the recovered C defect transformed into two C2 defects. There is one buckled dimer in between the two C2 defects, at the location where the protrusion of the C defect was located. No transition was observed after this.

### 3.2. Electronic structure of the C and C2 defects

We have measured the tunneling  $I$ - $V$  characteristics (as shown in the insets of Fig. 2) of the defects at each stage before and after the transitions displayed in Fig. 1 to investigate the electronic characteristics of the defects. Not only every C defect but also every C2 defect observed here showed a similar metallic feature. Each time the tunneling  $I$ - $V$  characteristics of the dimers were measured with the same tip apex and showed a semiconducting feature with a band gap of  $-0.5 \text{ V}$ , a result in accordance with previous

results. Tunneling spectra of the dimers were taken to confirm that the STS measurements were not influenced by the electronic structure of the tips, as mentioned in the following.

In the range from  $-2$  V to  $+2$  V, the normalized tunneling conductivities [STS spectra,  $(dI/dV)/(I/V)$  versus  $V$ ] were calculated numerically from the tunneling  $I$ - $V$  curves. The corresponding STS spectrum of each structure of the C defect shown in Fig. 1 is displayed in Fig. 2. Fig. 2a is the spectrum taken on top of the original C defect (C defect on the right side in Fig. 1a), Fig. 2b is the spectrum of the C2 defect in Fig. 1b, Fig. 2c the spectrum of the recovered C defect in Fig. 1c, Fig. 2d is a spectrum of another C defect (not shown) measured with the same tip apex, and the spectra of the dimers taken before (Fig. 2e) and after (Fig. 2f) the measurements of the defects are given for comparison and to justify the reliability of our STS measurements.

The normalization procedure of the tunneling current considerably emphasizes the tunneling noise (ca. several pA) around the Fermi level, preventing observation of the intrinsic electronic structure near the Fermi level. The shaded regions in Fig. 2 represent the energy window in which no reliable STS signals could be obtained because of the emphasized tunneling noise. We have relied on the tunneling  $I$ - $V$  curves shown in the insets of Fig. 2 and the non-normalized spectra (the  $dI/dV$  versus  $V$  curves, not shown) to determine whether the measured target is metallic or semiconducting.

The original C defect showed a metallic electronic structure in a similar fashion as reported before. Its electronic structure is characterized by one wide state located above the Fermi level spanning from  $-1$  V to  $\sim 1$  V with an intensity above  $\sim 3$  (the exact intensity cannot be estimated because it is located just above the Fermi level). This state is the origin of the appearance of the C defects as bright protrusions in STM images taken at low biases.

Surprisingly, the electronic structure of the C2 defect is almost the same as that of the C defect. It shows a metallic feature, and is characterized by one wide state located above the Fermi level. When the difference in their appearance in STM images is considered, this is surprising. The sim-

ilarity in the electronic structure suggests that the C2 defect is a variation of the C defect having a similar atomic structure.

Close inspection of the electronic structures of the original C defect and the recovered C defect shows that some differences exist between them in the filled states. While the original C defect shows a dip in intensity of the states around  $-1$  V, the intensity of the states of the recovered C defect remains approximately flat in the filled states in the regime of  $-2$  to  $-0.5$  V. This difference is readily observable in the STM images of Fig. 1 taken at a surface voltage of  $-1$  V (the bias at which the difference is most eminent), and the recovered C defect appears brighter than the original C defect, in accordance with the STS measurements. Fig. 2d shows an STS spectrum of another C defect located 20 nm to the right of the C defects displayed in Fig. 1. The electronic structure of this C defect is exactly the same as that of the recovered C defect, a result which suggests that C defects of this type are not peculiar and unique. This observation implies that there exists several (at least two) types of akin C defects having a very similar electronic structure. The difference in intensity between the original and recovered C defects might be related to the fact that the two defects act as different phase defects on the surrounding dimers.

Finally, we address the reliability of the STS measurements. It is well known that STS measurements are subject to the condition of the tunneling tip. A given tip apex will provide reproducible STS spectra, although a different tip apex might provide quite different spectra [8,9]. Regarding this point, each time (before and after the transitions) STS measurements were carried out on the dimers and we checked that each STS spectrum had a similar shape to the spectrum reported by Hamers et al. [10]. Representative spectra of the dimers measured before and after the structural transitions are displayed in Fig. 2e and f, respectively. Note that they are almost identical and have a similar shape to that reported by Hamers et al. [10] showing a semiconducting feature. The spectrum of the dimers obtained by Hamers et al. [10] (and thus ours) is consistent with many experimental results and is believed to represent the true electronic characteristics. By this procedure we can

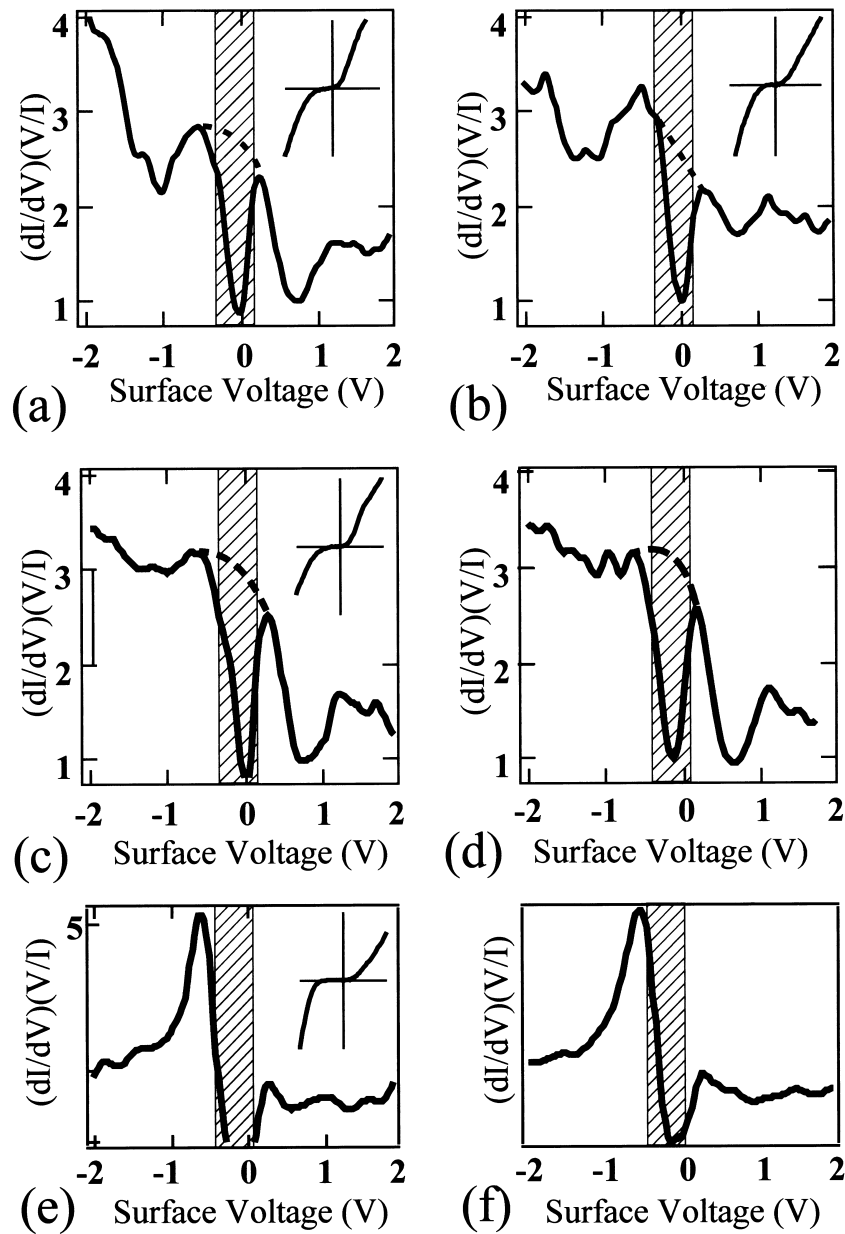


Fig. 2. STS spectra of the C defects. (a) STS spectrum of the C defect indicated by the arrow in Fig. 1a. (b) STS spectrum of the C2 defect in Fig. 1b. (c) STS spectrum of the recovered C defect in Fig. 1c. (d) STS spectrum of another C defect not shown in the STM images, taken during the measurements with the same tip apex. (e) STS spectrum of the dimers taken before the measurements of (a)–(d). (f) STS spectrum of the dimers taken after the measurements. Insets in the images show the tunneling  $I-V$  curve in the vicinity of the Fermi level in the range of  $-1$  V to  $+1$  V. The C defects show a metallic characteristic while the dimers are semiconducting.

safely confirm that all of the STS measurements are carried out under the same tip conditions and that the experimental results are not devalued by the possible electronic structure of the tips.

#### 4. Discussion

All of the experiments can consistently be understood if we interpret that the C2 defect is a metastable and excited state of the C defect. Direct observation of the C2→C defect transition is most important, since it excludes the possibility of the C→C2 defect transition being an irreversible and one-way structural transformation. Also, several other observations support this point: (1) when a particular surface area is scanned by STM for the first time, usually no or only a small number of C2 defects is observed in the area; and (2) the number of C2 defects observed in the scanned area increases gradually with repeated scanning.

The characteristics of the observed dynamic transition of the C defect provide many important implications concerning the atomic structure of the C defect. In this section we discuss this point, and propose a simple structure model of the C defect. High-resolution STM images of the C2 defect are displayed in Fig. 3 to show the dependence of the appearance of the C2 defect on surface bias. Fig. 3a is a filled-state image and Fig. 3b an

empty-state image. Since the surface bias is relatively low ( $-1$  V and  $0.6$  V) the states near the Fermi energy is probed, and thus the two protrusions of the C2 defect appear brighter than the surrounding dimers, in accordance with their metallic feature. Immediately it is apparent from Fig. 3 that the two bright protrusion of the C2 defect are observed exactly at the same location in the same way in the filled- and empty-state images. This means that the two bright protrusions do not originate from electronic modulation but are real topographic protrusions, and we assume each of them to be single atoms. Since these protrusion atoms easily move to the other side of the dimer row which always appears dark in the STM images, we conclude that the dark side is a real topographic vacancy. Considering this discussion we propose a simple structure model of the top layer of the C defect. Top layer of the C defect is composed of two atoms aligned side by side in the dimer row direction which appear as bright protrusions in the empty-state STM image, and the other side which always appears dark in the STM images is a real vacancy. This concept is consistent with the non-contact atomic force microscopy observations of Si(001) taken by Kitamura et al. [11], where the C defects were observed as two atoms missing along the dimer row. Since the top two atoms easily move to the opposite of the dimer row, we assume that they are somewhat weakly bound to

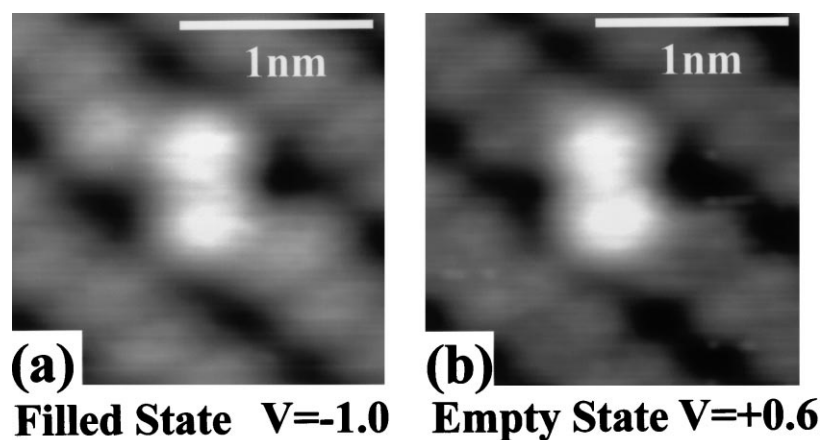


Fig. 3. High-resolution STM images of the C2 defects. (a) An STM image of the filled states; surface bias =  $-1.0$  V, tunneling current  $1$  nA. (b) An STM image of the empty states; surface bias =  $+0.6$  V, tunneling current  $1$  nA.

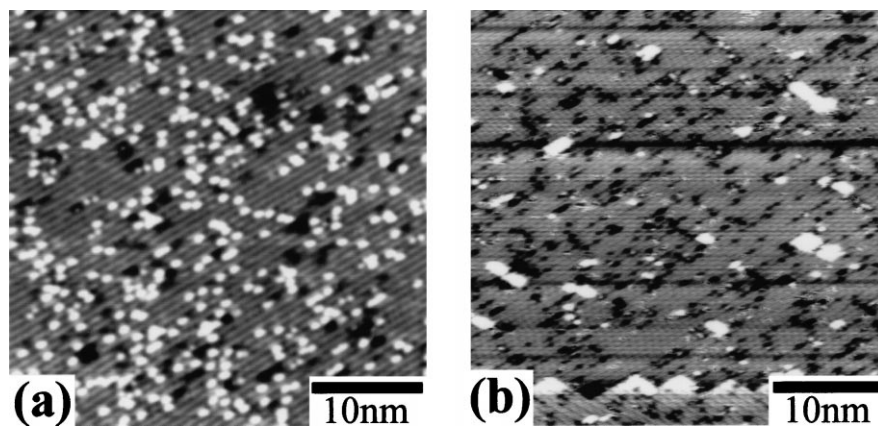


Fig. 4. (a) Empty-state STM image of a surface with a high density of C defects. Surface bias = +0.6 V, tunneling current 1 nA. (b) In situ empty-state STM image at approximately 200°C (estimated value from the power supply). The substrate was annealed by direct current and, as a result, the tunneling gap voltage is larger than the surface bias. Surface bias = +0.6 V, tunneling current 1 nA.

the second layer. Many other experimental observations are consistent with the notation of weakly bound top-layer atoms: (1) the top atoms are easily removed by perturbing the C defect with the STM tip [12]; and (2) vibration of the top two atoms induced by the tunneling tip was observed [12]. Our interpretation is that a metastable C defect is observed when these weakly bound atoms of the top layer move and are trapped in other configurations than the ground state. At the extreme case, one of the atoms slides to the opposite side of the dimer row inducing a structural transformation and the C defect is observed as a C2 defect.

Direct evidence of weakly bound top-layer atoms comes from an in situ observation of a surface with a high density of C defects at high temperatures. Fig. 4a shows an empty-state STM image of an Si(001) surface which has a high density of C defects. White protrusions observed in this image were confirmed to be C defects by an STM observation of the filled states (not shown). This surface was annealed at approximately 200°C and an in situ STM observation was carried out as shown in the empty-state STM image of Fig. 4b. The C defects have disappeared and instead islands with monolayer height and many dark vacancies are observed. The islands are elongated in the direction perpendicular to the

surface dimer rows. A close inspection of the islands shows that they are composed from dimers with a  $\times 2$  periodicity. Islands formed by deposition of silicon on Si(001) show the same feature [13,14] and we assume that the islands observed on the annealed surface are also composed of silicon. The density of the dark vacancies observed on the annealed surfaces and that of the C defects on the initial surface are the same, thus we conclude that the dark vacancies are remnants of the C defects. Regarding this experiment, we interpret that the element of the two atoms in the top layer is silicon, and that they are weakly bound to the second layer.

The vacancies observed in the in situ STM image of Fig. 4b might not be real vacancies as they were not buried at high temperature. We assume that there is an extrinsic atom at the second layer beneath the top two silicon atoms which is observed as the vacancy at high temperature. The extrinsic atom can be regarded as the origin of the C defect. We reached this conclusion by observing that the density of the C defects increases with exposure time in vacuum, as shown in a set of STM images of a surface taken at different durations after flashing in Fig. 5. Fig. 5a–c are empty-state STM images taken 30 min, 4 h and 8.5 h after flashing, respectively. Fig. 5d and e show the dependence of the STM image of the surface

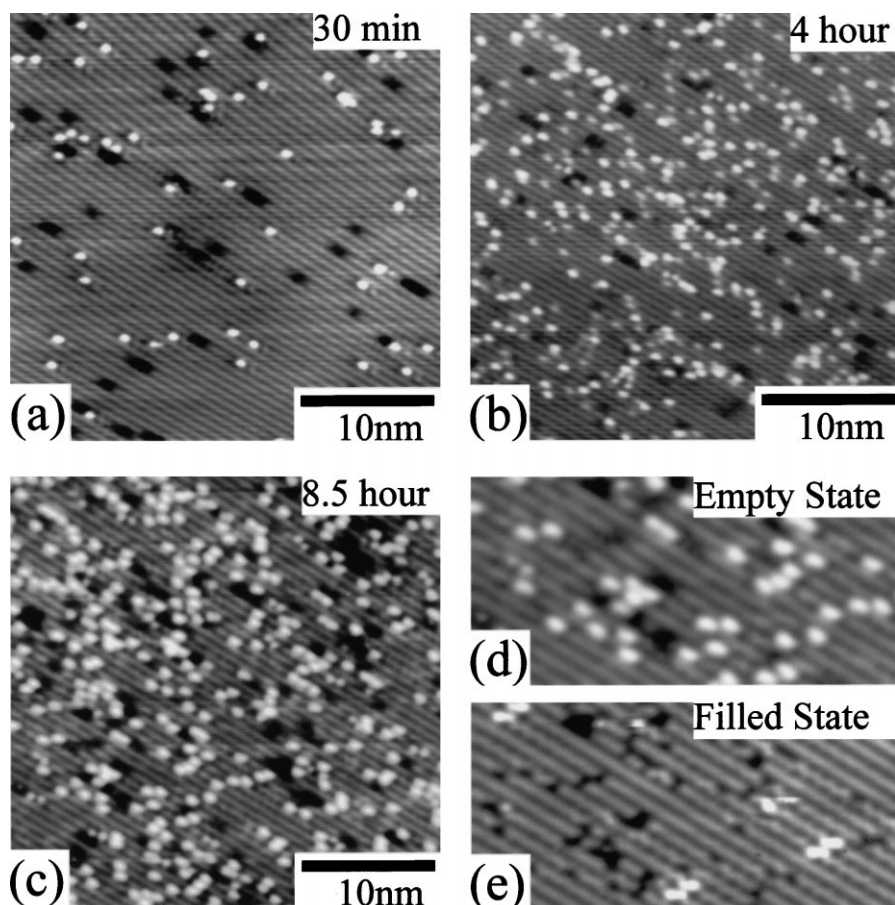


Fig. 5. A set of STM images of a surface taken at different times after flashing. (a), (b), and (c) are empty-state STM images taken 30 min, 4 h and 8.5 h after flashing, respectively. Surface bias = +0.6 V, tunneling current 1 nA. (a) to (c) are not a result of a sequential observation, and each image was taken at a different location on the surface. (d) Empty (surface bias = +0.6 V, current 1 nA) and (e) filled (surface bias = -1.5 V, current 1 nA) state STM images of the same location on the surface 8.5 h after flashing.

exposed to vacuum for 8.5 h on surface bias, taken to check that the protrusions observed in the empty-state STM image of Fig. 5a–c show the characteristics of the C defects in the filled-state images. It is clear that the density of the C defect increases with time after flashing. Zhang et al. have observed an occasional generation of a new C defect during STM imaging, and have suggested that the C defects could be induced from some remaining stress generated by the preceding flashing treatment [3]. Since we observed that the rate of increase of the C defects with time depends strongly on the vacuum pressure, where a high base pressure gives a lower increase rate, we con-

clude that the C defects are not induced by the stress but are induced by extrinsic atoms which exist in typical vacuum conditions. Further support for the concept of an extrinsic atom beneath the top layer comes from an observation that perturbing the C defect by the tunneling tip never left a clean and complete silicon surface, although the remnant was almost always a vacancy that was not able to be removed [13].

In Fig. 6 we summarize the above discussions and show a rough sketch of the proposed structure of the C defect. An extrinsic atom exists in the second layer, and two atoms (most likely to be silicon) are weakly bound to this extrinsic atom.

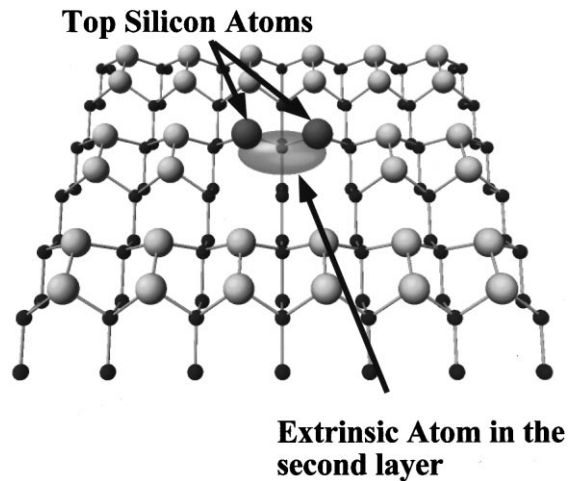


Fig. 6. A schematic model of the proposed structure of the C defect. The two top and black circles represent the top two atoms that are likely to be silicon and the oval shape represents the extrinsic atom which lies in the second layer. See text for details.

By this simple though reasonable structure it is possible to explain many observed characteristics of the C defect. Further studies, especially theoretical calculations, are required to elucidate the element of the extrinsic atom and to elucidate the details of the atomic structure of the C defect.

## 5. Conclusion

In conclusion, the dynamic features of the C defect were studied by consecutive STM/STS observations. Both the C to C2 transition and the reverse C2 to C transition were observed. STS measurements revealed that the electronic structure of the C2 defect is almost identical to that of the C defect, even though their topographical structures are quite different. We assume that the C2

defect is a metastable and excited state of the C defect. We propose a rough sketch of the still unidentified atomic structure of the C defect. By means of this model, it is possible to explain many experimentally observed features of the C defect.

## Acknowledgements

This work was supported by the Shigekawa Project of TARA, University of Tsukuba. The support of a Grant-in-Aid for Scientific Research from the Ministry of Education, Science and Culture of Japan is also acknowledged.

## References

- [1] R.M. Tromp, R.J. Hamers, J.E. Demuth, *Phys. Rev. Lett.* 55 (1985) 1303.
- [2] R.J. Hamers, U.K. Kohler, *J. Vac. Sci. Technol. A* 7 (1989) 2854.
- [3] Z. Zhang, M.A. Kulakov, B. Bullemer, *Surf. Sci.* 369 (1996) L131.
- [4] Ph. Avouris, D. Cahill, *Ultramicrosc.* 42–44 (1992) 838.
- [5] V.A. Ukraintsev, Z. Dohnalek, J.T. Yater, *Surf. Sci.* 388 (1997) 132.
- [6] M. Udagawa, Y. Umetani, H. Tanaka, M. Itoh, T. Uchiyama, Y. Watanaba, T. Yokotsuka, I. Sumita, *Ultramicrosc.* 42–44 (1992) 946.
- [7] H. Ikegami, K. Ohmori, H. Ikeda, H. Iwano, S. Zaima, Y. Tasuda, *Jpn. J. Appl. Phys.* 35 (1996) 1593.
- [8] J.P. Pelz, *Phys. Rev. B* 43 (1991) 6746.
- [9] T. Klitsner, R.S. Becker, J.S. Vickers, *Phys. Rev. B* 41 (1990) 3837.
- [10] R.J. Hamers, Ph. Avouris, F. Bozso, *Phys. Rev. Lett.* 59 (1987) 2071.
- [11] S. Kitamura, K. Suzuki, M. Iwatsuki, *Jpn. J. Appl. Phys.* 37 (1998) 3765.
- [12] K. Hata, M. Ishida, K. Miyake, H. Shigekawa, *Appl. Phys. Lett.* 73 (1998) 40.
- [13] Y.-W. Mo, B.S. Swartzentruber, R. Kariotis, M.B. Webb, M.G. Lagally, *Phys. Rev. Lett.* 63 (1989) 2393.
- [14] Y.W. Mo, J. Kleiner, M.B. Webb, M.G. Lagally, *Phys. Rev. Lett.* 66 (1991) 1998.